Cone-shaped socket connections for cylindrical members

H. Kuwamura[1] & T. Ito[2]

[1]*Department of Architecture, The University of Tokyo, Tokyo, Japan*

[2]*Department of Architecture, Tokyo University of Science, Tokyo, Japan*

ABSTRACT: A new connection method, which is called cone-to-cylinder socket connection, is developed in Japan in order to facilitate connecting a circular hollow section member to another cylindrical or different shaped section member. The apex part of a cone is inserted into the open mouth of a cylinder, and then a connected member is placed on the foot of the cone. In general, a lid plate is attached in advance to the foot of the cone in order to serve as a splice to fix the connected member. The benefit expected in this socket connection is that field connection of struts or piles of cylindrical section with other structural members such as beams and foundations is substantially simplified. In addition, when the wall of the cone is metal-touched with the inner circular edge of the cylinder, the connection can be assumed a pin-support or pin-node in all directions, which reduces the stresses in the connected members. Compression test of typical assembles of the socket connection demonstrated that the socket has sufficient strength and stiffness, even though the thickness of the cone is only 4.5mm. It was also shown that yield, plastic, and ultimate loads of the socket can be predicted by the bending theory of shells.

1 GENERAL INFORMATION

1.1 *The cone-to-cylinder socket connection*

A new connection method, which is called cone-to-cylinder socket connection, is developed in Japan in order to facilitate connecting a circular hollow section member to another cylindrical or different shaped section member. As shown in Figure1, the apex part of a cone is inserted into the open mouth of a cylinder, where the foot diameter of the cone is larger than the inner diameter of the cylinder, and then a connected member is placed on the foot of the cone. In general, a lid plate is attached in advance to the foot of the cone in order to serve as a splice to fix the connected member. Experimental test and numerical analysis on the socket connection conducted by Steel Structural Laboratory, the University of Tokyo revealed that the connection is strong and rigid enough to be applied to construction practice of low to middle-rise buildings (Kuwamura et al. 2005a,b, Tomioka et al. 2006, Ito et al. 2008).

1.2 *Expected applications of the socket*

The benefit expected in this socket connection is that field connection of struts or piles of cylindrical section with other structural members such as beams and foundations is substantially simplified as sketched in Figure 2. In addition, when the wall of the cone is metal-touched with the inner circular edge of the cylinder, the connection can be assumed a pin-support or pin-node in all

directions (Kuwamura & Ito 2007). This is a great advantage of the connection, because such a pin-joint substantially reduces the stresses in the cylindrical piles and mitigates the damages by a severe earthquake, which were largely observed in pile foundations in Kobe by the 1995 Hanshin-Awaji Earthquake Disaster. From this point of view, an application of the cone to the connection of steel piles and foundation beams in house buildings is studied in practice by house builders.

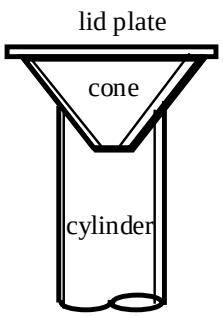

Figure 1. Socket connection

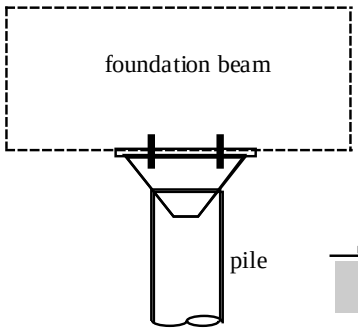

(a) pile cap

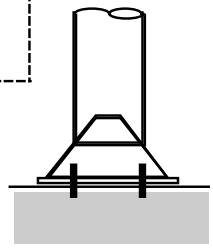

(b) column base

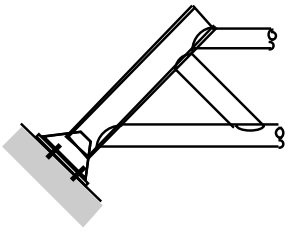

(c) truss support

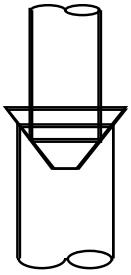

(d) pipe joint

Figure 2. Application of socket connection

1.3 *Scope of this paper*

In this paper, experimental test results of the socket connections are presented focusing the most important behavior when the socket is subjected to uniform compressive load. The test data were extracted from a series of tests with more than a hundred specimens (Kuwamura et al. 2005a, Tomioka et al. 2006). It is also shown the load carrying capacity is predicted from bending theory of shells.

2 EXPERIMENTS

2.1 *Specimen*

The number of specimens introduced here is only 5, which are representative specimens designated by No.1, No.3, No.5, No.8, and No.11. They are picked up from the data of more than 100 specimens above mentioned. The shape and construction of each specimen are shown in Figure 3. Each specimen is assembled from a short cylindrical pipe, a cone inserted into the open mouth of the cylinder, a square lid plate on the cone, and a circular ring to strengthen the cylinder edge. The ring is furnished only to No.5 and No.11. The joint between the cone and lid is metal-touched for No.1, No.3, and No.11, but welded for others. The joint between the cylinder and cone is metal-touched for No.1 No.5, and No.11, but welded for others. This parametric scheme is shown in Table 1. Other physical conditions are the same for all the specimens as shown in Figure 3. It will be noticed that the apex angle of the cone is 90 degree in these five specimens and that the nominal thickness of the cone is only 4.5 mm.
All of the materials employed to the cylinder, the cone, the lid, and the ring are mild steels with a nominal tensile strength of 400MPa. They are designated by SS400 for plate, STK400 for cylinder. The mechanical properties obtained from laboratory coupon tests are shown in Table 2. The cone is formed from the plate of SS400 by cold bending, and then seam-welded.

2.2 *Loading*

Each specimen is loaded by central compression through a rigid piston-head of test machine as shown in Figure 3. Thus, uniform pressure is applied to the upper edge of the cone through the lid plate. The load is quasi-statically applied and the relative displacement between the piston head and the test bed are successively measured. The loading is stopped when the maximum load is attained and further sufficient deformation due to damage is observed.

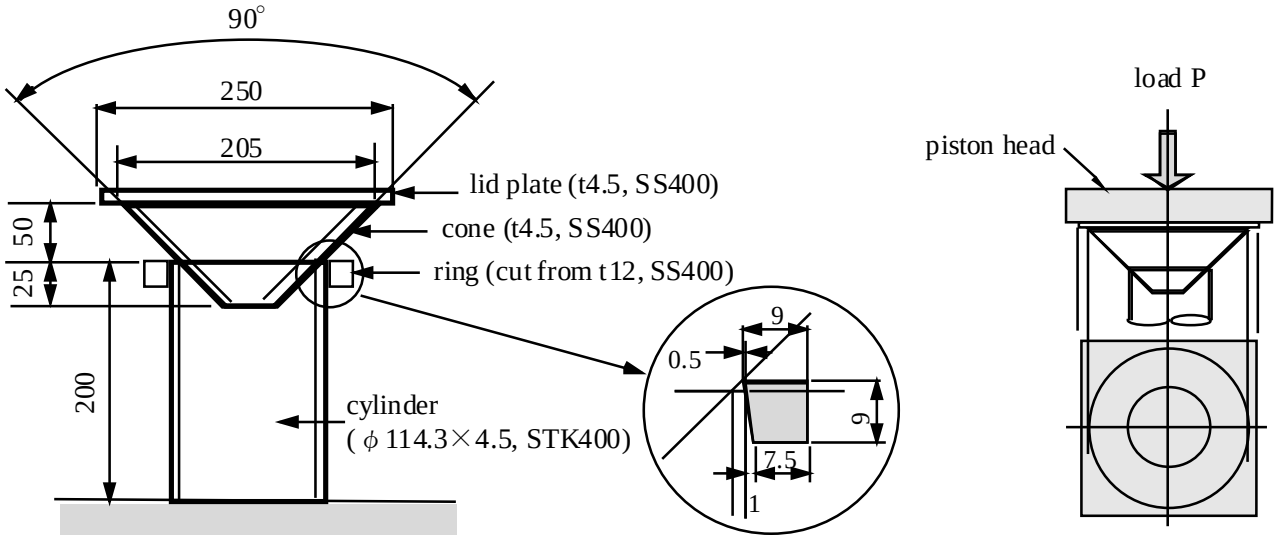

Figure 3. Specimen setup and loading

Table 1. Experimental conditions and results

Specimen No	conditions			results						
	cone to lid	cone to cylinder	ring	failure mode	yield load (kN)	plastic load (kN)	max load (kN)	stiffness (kN/mm)	play (mm)	remarks
1	metal touch	metal touch	none	CyE→CoE	88 (232)	141	171 (288)	175	0.3	Values in parentheses are for CoE-mode.
3	metal touch	weld	none	CoE	158	227	239	291	0.2	
5	weld	metal touch	furnished	CoB	142	222	304	265	0.3	RiT-mode is sligtly mixed.
8	weld	weld	none	CoBu	275	406	424	762	0.5	
11	metal touch	metal touch	furnished	CoE	120	-	180	155	0.5	

Table 2. Material Properties

steel	thickness (mm)		yield strength	tensile strength	uniform elongation	remarks
	nominal	measured	(N/mm^2)	(N/mm^2)	(%)	
SS400	4.5	4.18	333	419	17	cone, lid
SS400	12.0	10.2	305	460	19	ring
STK400	4.5	4.73	320	376	11	cylinder

2.3 *Failure mode*

Five modes of failure shown in Figure 4 are anticipated. The symbol 'CyE' indicates 'Cylinder Edge failure' like a trumpet, which is associated with the sinking of the cone into the interior of the cylinder. 'CyE' is expected to occur only in the case that the cone and the cylinder are metal-touched without welding. 'CoE' indicates 'Cone Edge failure', which is expected to occur only in the case that the cone is metal-touched with the lid plate. 'CoB' indicates 'Cone Bending faifure', and 'CoBu' indicates 'Cone Buckling failure', but it may be difficult to distinguish 'CoB' and 'CoBu' in the plastic behavior. 'RiT' indicates 'Ring Tension failure', which is obviously

anticipated for the cylinder furnished with the ring where the cylinder is not welded to the cone. The reality of the failure mode observed in the experiment is given in Table 1, and the configurations of the specimens after test are shown in Figure 5. In the specimen No.1, 'CyE' was first observed and then 'CoE' governed the final stage. 'RiT' was not visually observed, but was possible in No.5.

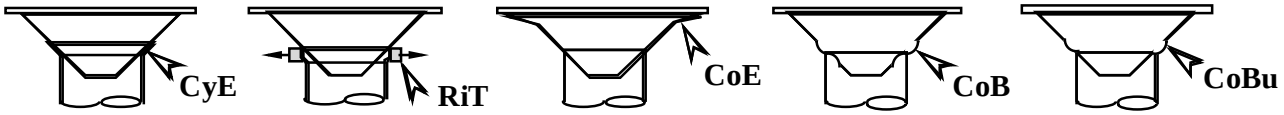

Cylinder-Edge Failure | Ring Tension Failure | Cone-Edge Failure | Cone Bending Failure | Cone Buckling Failure

Figure 4. Failure modes

Figure 5. Failure deformation after test

2.4 *Load-displacement curve*

The relationships between compressive load and axial shortening are shown in Figure 6. The specimens No. 1 and No.11 have two peaks in their load-displacement curve. In No.1, the first peak is due to the mode 'CyE', and the second peak is 'CoE' as mentioned above. In No. 11, both peaks are due to 'CoE', which are attributed to different states of equilibrium in small deformation and large deformation.

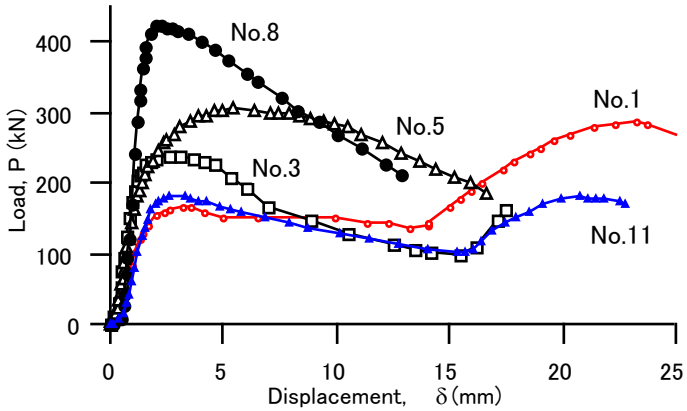

Figure 6. Load-displacement curves from experiment

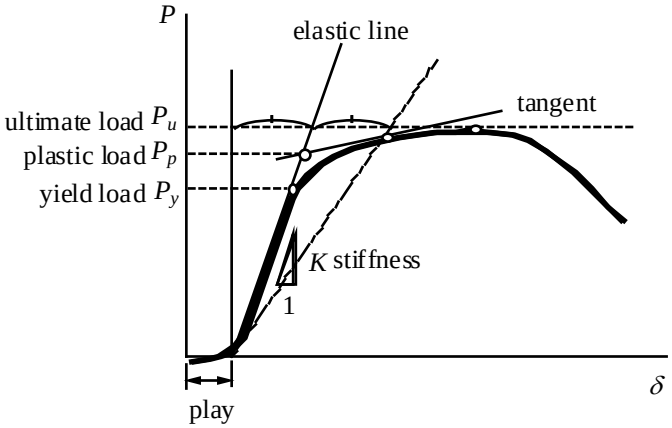

Figure 7. Standard load-displacement curve and definition of strength and stiffness

The load-displacement curve of the socket connection is generally drawn like the curve of Figure 7. This defines several important properties: the play at the initial stage of loading which comes from some inevitable looseness between the elements constituting the connection, the elastic line which gives the stiffness of the connection, the yield load which serves as the strength limit of allowable stress design, the plastic load which serves as the strength limit of plastic design, and the ultimate load which serves as the safety margin for extreme loading condition in abnormal situation. These properties are summarized in the above Table 1.

2.5 *Remarks on experimental results*

The strongest one among the five is No.8 that has welds at the joint of cone and lid as well as of cone and cylinder, but its behavior after the maximum load is less ductile than others, because the ultimate load is somewhat related to the shell buckling. The yield load governed by 'CyE' is fairly low as known from 88kN of No.1, but this type of failure is easily restrained by the ring such that the yield load is 142kN of No.5 or 120kN of No.11. This means that the weakest point in this socket connection without weld lies in the free edge of the cylinder. Since it is not economical to increase the thickness of the cylindrical member to get a higher CyE-strength, the ring or weld is a better choice. The second weakest lies in the upper free edge of the cone as observed in No.11. This suggests that the cone should be welded to the lid plate in advance, which seems more convenient in the practice of construction. In practical view point, all these specimens seem to be applicable to the pile heads of low-rise residential houses, because the vertical load at the column base is not more than 50kN in such buildings, which is exceeded by the yield loads of all specimens.
The play at the initiation of loading is not more than 0.5 mm, which is small enough to avoid an error in site construction. The elastic stiffness is sufficiently large such that the shrinkage of the connection is less than 0.3 mm under the load of 50kN.

3 THEORETICAL ANALYSIS

3.1 *Bending failure of cylinder edge*

The yield, plastic, and ultimate loads for the cylinder edge failure 'CyE' were theoretically analyzed by Kuwamura et al. (2005b). The solutions are as follows:

$$P_y = A_p \sigma_{yp} \frac{2a_1 \beta^3 D_p}{E t_p} \cdot \frac{\tan\alpha + \mu}{1 - \mu \tan\alpha} \tag{1}$$

$$P_p = P_y + A_p \frac{{\sigma_{yp}}^2}{E} \left(n_p - 1\right) \cdot \frac{1 + \mu \cot\alpha}{1 - \mu \tan\alpha} \tag{2}$$

$$P_u = P_y + A_p \frac{\sigma_{yp}}{E} \cdot \frac{\sigma_{yp} + \sigma_{up}}{2} \left(n_u - 1\right) \cdot \frac{1 + \mu \cot\alpha}{1 - \mu \tan\alpha} \tag{3}$$

where

$$\beta = \sqrt[4]{\frac{3\left(1 - \nu^2\right)}{{a_1}^2 {t_p}^2}}, \text{ and } D_p = \frac{E {t_p}^3}{12\left(1 - \nu^2\right)} \tag{4}$$

Other symbols are defined in Figure 8. The yield load is derived from the bending theory of a circular cylinder subjected to axially symmetrical load. The plastic load that assumes a band pressure as shown in Figure 9 is different from the solution by Eason and Shield (1955) which assumes a line load. The strain hardening factors n_p and n_u are properly defined from the observation of the stress-strain relation of the material of the cold-formed cylinder, so that n_p=15 and n_u=70 (Kuwamura et al. 2005b). The calculated values of strength are shown in the column CyE of Table 3 for several possible values of the friction coefficient μ. Comparing the calculation with the experimental results of No.1, the calculation is adequate for the friction coefficient ranging from 0.2 to 0.3, which is the normal value often observed at the contact between steel and steel.

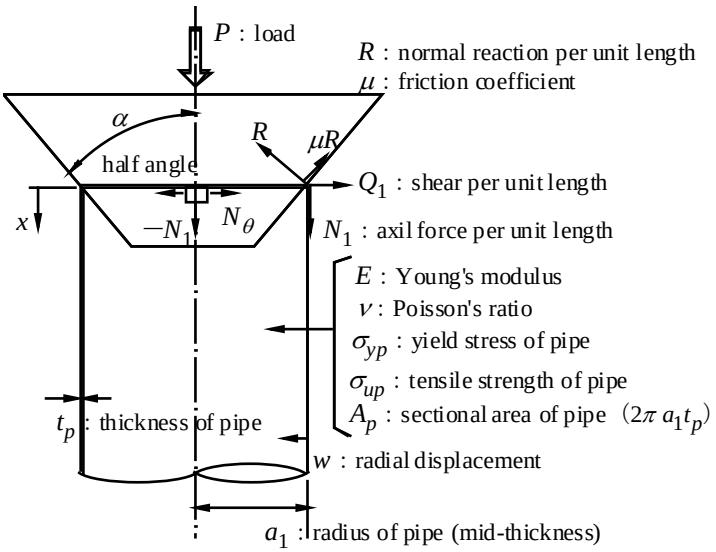

Figure 8. Symbols for cylinder edge failure

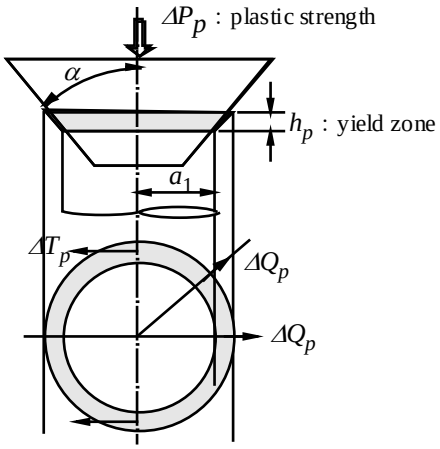

Figure 9. Yield zone for cylinder edge failure

Table 3. Comparison of analytical and experimental values of yield, plastic, and ultimate loads

CyE				CoE				CoB			
friction coef.	Py (kN)	Pp (kN)	Pu (kN)	friction coef.	Py (kN)	Pp (kN)	Pu (kN)	friction coef.	Py (kN)	Pp (kN)	Pu (kN)
0.0	60	71	121	0.0	87	143	179	0.9	131	196	246
0.1	73	87	147	0.1	97	159	199	1.0	137	206	259
0.2	89	106	181	0.2	109	179	224	1.1	144	216	272
0.3	111	132	224	0.3	124	204	256	1.2	151	227	285
0.4	139	166	281	0.4	145	238	298	1.3	158	237	298
				0.5	174	286	358	1.4	165	247	311
No.1	88	141	171	No.3 (No.11)	158 (120)	227 (-)	239 (180)	No.5	142	222	304

3.2 *Tension failure of ring*

The yield, plastic, and ultimate loads for the ring tension failure 'RiT' were also theoretically analyzed by Kuwamura et al. (2005b). But here they are skipped, because reference test data is absent in the five specimens.

3.3 *Bending failure of cone edge*

The yield, plastic, and ultimate loads for the cone edge failure 'CoE' were also theoretically analyzed by Kuwamura et al. (2005b). The yield load is based on the elastic bending theory of a cone. Since the equations for calculating the yield load is very lengthy, only the basic idea is explained herein. The stresses and displacements shown in Figure 10 of a cone subjected to axially symmetrical load are solved by Flugge (1973) and Timoshenko et al. (1959), and their values are determined by the following boundary conditions with the reference of Figure 11:

$$Q_s = -\frac{P}{2\pi a_2}(\sin\alpha - \mu\cos\alpha) \quad \text{and} \quad M_s = 0 \quad \text{at} \quad s = s_2 \tag{5}$$

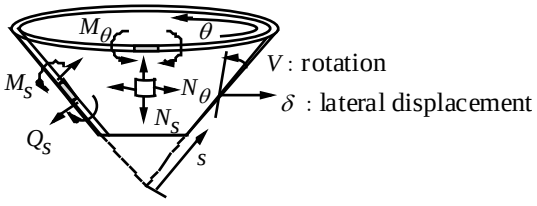

Figure 10. Stresses and displacements of a cone

Then assuming the following simplified yield criterion,

$$N_\theta = \sigma_{yc}\, t_c \quad \text{at} \quad s = s_2 \tag{6}$$

we obtain the yield load *Py* when the upper free edge of the cone yields.
The plastic and ultimate loads are based on the plastic zone shown in Figure 12, and are given by

$$P_p = 2\pi \frac{\sigma_{yc} t_c^{\,2}}{4} \cdot \frac{\tan\alpha}{\tan\alpha - \mu}\left(2\sqrt{\frac{2s_2}{t_c \tan\alpha}} - 1\right) \tag{7}$$

$$P_u = P_p \frac{\sigma_{uc}}{\sigma_{yc}} \tag{8}$$

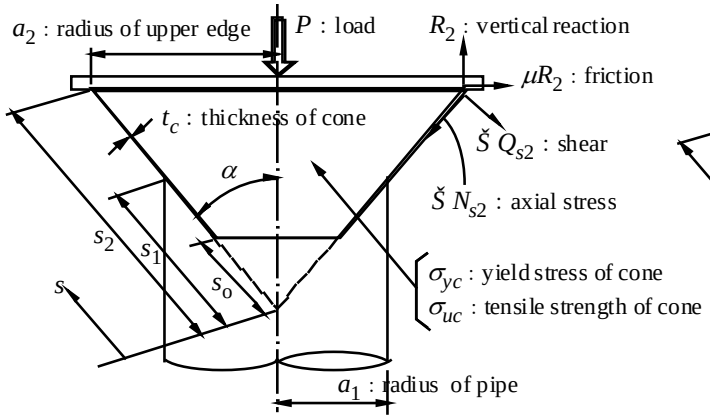

Figure 11. Symbols for the analysis of cone edge failure

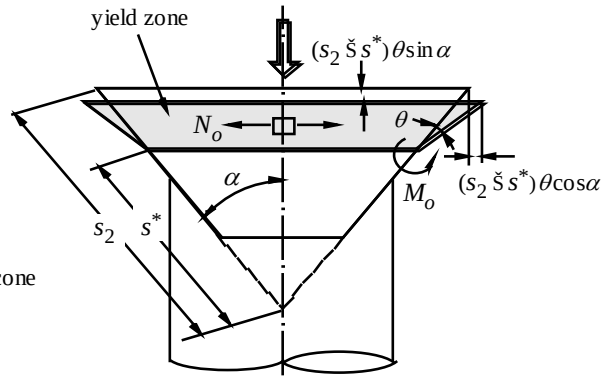

Figure 12. Plastic zone of upper cone

The above analytical solutions are compared with the test results of specimen No.3 in the column of 'CoE' of Table 3. The calculation is adequate for the friction coefficient ranging from 0.2 to 0.4. Noticing that specimen No.11 is less strong than specimen No.3, both of which have the same failure mode 'CoE', the boundary of the lower part of the cone has some influence on the strength, but this is not incorporated in the above theoretical solutions.

3.4 *Bending failure of cone wall*

The yield, plastic, and ultimate loads for the bending failure of cone wall, i.e., 'CoB' mode were analyzed by Kuwamura et al. (2005b). The yield load is also based on the bending theory of a cone above mentioned, in which following five boundary conditions are employed with the notations in Figures 10 and 13:

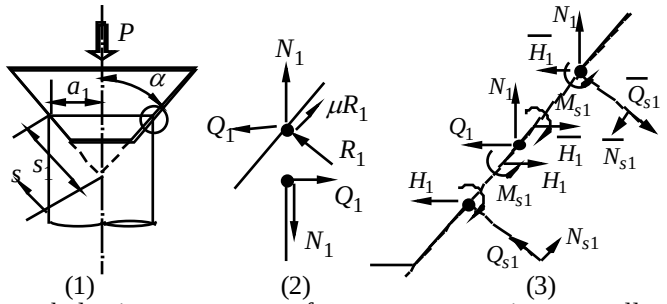

Figure 13. Symbols for the bending failure of cone wall

$$Q_{s1} - \overline{Q}_{s1} = \frac{P}{2\pi a_1} \cdot \frac{1}{\sin\alpha + \mu\cos\alpha} \tag{9}$$

$$M_{s1} = M_s, \qquad \overline{M}_{s1} = M_s, \qquad \delta_1 = \overline{\delta}_1, \qquad V_1 = \overline{V}_1 \tag{10}$$

With the following simple yield criterion:

$$M_s = \sigma_{yc} \frac{t_c^{\,2}}{6} \tag{11}$$

we obtain the yield load P_y. The plastic and ultimate loads are

$$P_p = 1.5P_y, \qquad P_u = \frac{\sigma_{uc}}{\sigma_{yc}} P_p \tag{12}$$

The calculated loads are compared with the data of No.5 in the column of 'CoB' of Table 3. In this case large friction coefficient is favorable, because the expansion of the cone due to Poisson's ratio makes the cone sit on the edge of the cylinder.

3.5 *Buckling failure of cone wall*

It is known that the elastic buckling strength of a cone is equal to that of a cylinder which has the same curvature as the principal curvature of the cone (Seide 1596). Thus the buckling strength of an elastic cone is represented by the Donnell's formula by using $a/\cos\alpha$ instead of a. In this case of specimen No.8, however, the cone goes into the inelastic range, the Young's modulus should be modified. If Gerard's modification is applied, the inelastic buckling load of the cone is

$$\sigma_{cr} = \frac{\sqrt{E_t E_s}}{\sqrt{3(1-\nu^2)}} \cdot \frac{t_c \cos\alpha}{a} \tag{13}$$

Here the tangent modulus E_t and secant modulus E_s are simply assumed as

$$\frac{E_t}{E}, \frac{E_s}{E} = 1 - \frac{\sigma - 0.6\sigma_{yc}}{\sigma_{uc} - 0.6\sigma_{yc}} \tag{14}$$

we obtain the following explicit equation for the inelastic buckling strength of the cone:

$$P_{cr} = 2\pi a t_c \cdot \frac{\tau_o}{\kappa(\tau_o - 0.6) + 1/\sigma_{yc}}, \quad \text{where} \quad \kappa = \frac{a\sqrt{3(1-\nu^2)}}{E t_c \cos\alpha}, \quad \tau_o = \frac{\sigma_{uc}}{\sigma_{yc}} \tag{15}$$

Since the buckling wave is observed in the lower part of the cone above the cylinder, the radius a_1 of the cylinder is employed for a, we obtain P_{cr} = 414kN, which is close to the ultimate load 424kN of specimen No.8 with the failure mode 'CoBu'.

4 CONCLUSIONS

A new type of connection called cone-to-cylinder socket connection is introduced. This will serve to significantly facilitate the site construction of cylindrical members such as pile cap, base of pipe strut, support of pipe truss, and pipe-to-pipe joint. The compression test demonstrated this connection has enough strength and stiffness for the use in moderate scale of structures. The yield, plastic, and ultimate loads of the connection were analyzed by the bending theory of shells.

References

Eason, G. and Shield, R. T. 1955. The influence of free ends on the load-carrying capacities of cylindrical shells. *J. of Mechanics and Physics of Solids* 4:17-27.

Flugge, W. 1973. *Stresses in shells, 2nd Ed.* New York: Springer-Verlag.

Ito, T. and Kuwamura, H. 2008. Cylinder edge failure of steel cone-to-cylinder socket connections under compression. *J. Struct. Constr. Eng. AIJ* 73(630): 1377-1384.

Kuwamura, H., Ito, T., and Tomioka, Y. 2005a. Study on steel cone-to-cylinder socket connections. *Summaries of Tech. Papers of Annual Meeting of Arch. Ins. Japan* C-1: 887-892.

Kuwamura, H., Ito, T., and Tomioka, Y. 2005b. Study on steel cone-to-cylinder socket connections. *J. Struct. Constr. Eng. AIJ* 598: 155-162.

Kuwamura, H., Ito, T. 2007. Frictional rotation resistance of steel cone-to-cylinder socket connections. *J. Struct. Constr. Eng. AIJ* 622: 169-176.

Seide, P. 1956. Axisymmetrical buckling of circular cones under axial compression. *J. Applied Mechanics* 23(4): 625-628.

Timoshenko, S. and Woinowsky-Krieger, S. 1959. *Theory of plates and shells*. New York: McGraw-Hill.

Tomioka, Y., Ito, T., and Kuwamura, H. 2006. Study on steel pipe joints with an inserted cone, *Proc. 77th Arch. Res. Meeting of Kanto Chapter AIJ*: 145-148.